Food & Function

Accepted Manuscript

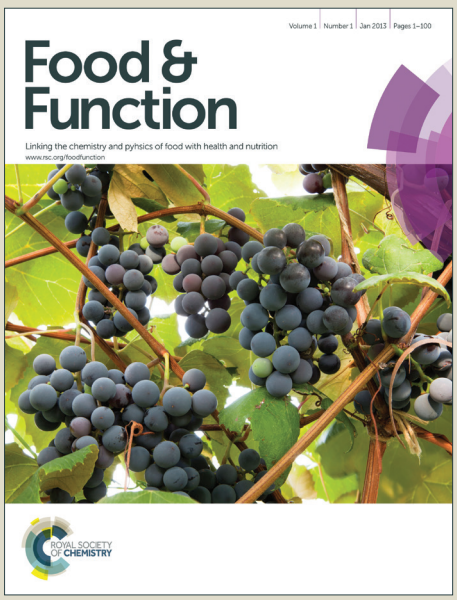

This is an *Accepted Manuscript*, which has been through the Royal Society of Chemistry peer review process and has been accepted for publication.

Accepted Manuscripts are published online shortly after acceptance, before technical editing, formatting and proof reading. Using this free service, authors can make their results available to the community, in citable form, before we publish the edited article. We will replace this *Accepted Manuscript* with the edited and formatted *Advance Article* as soon as it is available.

You can find more information about *Accepted Manuscripts* in the Information for Authors.

Please note that technical editing may introduce minor changes to the text and/or graphics, which may alter content. The journal's standard Terms & Conditions and the Ethical guidelines still apply. In no event shall the Royal Society of Chemistry be held responsible for any errors or omissions in this *Accepted Manuscript* or any consequences arising from the use of any information it contains.

ROYAL SOCIETY OF CHEMISTRY

www.rsc.org/foodfunction

Research Article

Antrodia camphorata induces G_1 cell-cycle arrest in human premyelocytic leukemia (HL-60) cells and suppresses tumor growth in athymic nude mice

Hsin-Ling Yang[a,†], K.J. Senthil Kumar[a], Ya-Ting Kuo[a], Hebron C. Chang[b,†], Jiunn-Wang Liao[c], Li-Sung Hsu[d], You-Cheng Hseu[e,f,*]

[a]*Institute of Nutrition, China Medical University, Taichung 40402, Taiwan*

[b]*Institute of Biotechnology and Bioinformatics, Asia University, Taichung 41354, Taiwan*

[c]*Graduate Institute of Veterinary Pathology, National Chung Hsing University, Taichung 402, Taiwan*

[d]*Institute of Biochemistry and Biotechnology, Chung Shan Medical University, Taichung 40401, Taiwan*

[e]*Department of Health and Nutrition Biotechnology, Asia University, Taichung 41354, Taiwan*

[f]*Department of Cosmeceutics, College of Pharmacy, China Medical University, Taichung 40402, Taiwa. E-mail addresses: ychseu@mail.cmu.edu.tw; Fax: +886 4 22078083; Tel.: +886 4 22053366x5308.*

[†] *Both authors contributed equally.*

ABSTRACT

Antrodia camphorata is a well-known medicinal mushroom in Taiwan. The broth from a fermented culture of *Antrodia camphorata* (AC) has been shown to induce apoptosis in cultured human premyelocytic leukemia (HL-60) cells. In the present study, we examined the effects of AC on cell cycle arrest *in vitro* in HL-60 cells and on tumor regression *in vivo* using an athymic nude mouse model. We found that AC (20–80 μg/mL) treatment significantly induced G_1 cell-cycle arrest in HL-60 cells by reducing the levels of cyclin D1, CDK4, cyclin E, CDK2, cyclin A, and phosphorylation of retinoblastoma protein (p-Rb). Moreover, AC treatment led to significantly increased protein expression levels of CDK inhibitors, including $p21^{WAF1}$ and $p15^{NIK4B}$. Additionally, AC treatment markedly induced intracellular ROS generation and mitochondrial dysfunction in HL-60 cells. Furthermore, the *in vivo* study results revealed that AC treatment was effective in terms of delaying the tumor incidence in nude mice that had been inoculated with HL-60 cells as well as reducing the tumor burden. Histological analysis confirmed that AC treatment significantly modulated the xenografted tumor progression as demonstrated by a reduction in mitotic cells. Our data strongly suggest that *Antrodia camphorata* could be an anti-cancer agent for human leukemia.

Introduction

Antrodia camphorata (AC) is a native Taiwanese medicinal mushroom, popularly known as "Niu Cheng Zhi" in Taiwan, that grows in the inner sap of the *Cinnamomum kanehira* Hay (*Lauraceae*) tree.[1] AC has been used in traditional Chinese medicine to treat food poisoning, drug intoxication, diarrhea, abdominal pain, hypertension, skin irritation, and cancer.[2] This medicinal mushroom has recently attracted interest because it possesses a number of bioactive components such as triterpenoids, polysaccharides, maleic/succinic acid derivatives, benzenoids, and benzoquinone derivatives.[3-5] Increasing evidence suggests that AC exhibits an extensive range of biological activities, including antioxidant, anti-inflammatory, hepatoprotective, antimetastatic, antihypertensive, antihyperlipidemic, immunomodulatory, and anticancer properties.[3-6] AC is a non-mutagenic mushroom with low toxicity that has been shown to efficiently reduce the tumorigenicities of various cancers *in vitro* and *in vivo*.[7]

Chemoprevention, which refers to the administration of natural or synthetic agents to prevent events associated with carcinogenesis initiation and promotion, is increasingly appreciated as an effective approach to neoplasia management.[8] Many studies have shown a clear link between abnormal cell cycle regulation or apoptosis and cancer, and cell cycle inhibitors and apoptosis-inducing agents are receiving appreciation as cancer management tools.[9,10] Eukaryotic cell cycle progression involves the sequential activation of cyclin-dependent kinases (CDKs), the activation of which depends upon their associations with cyclins.[11] Mammalian mitotic cycle progression is controlled by multiple holoenzymes that comprise a catalytic CDK and a cyclin regulatory subunit.[12] These cyclin-CDK complexes are activated at specific intervals during the cell cycle but can also be induced and regulated by exogenous factors. Cell cycle progression is also regulated by the relative balance between the cellular concentrations of cyclin-CDK complexes and CDK inhibitors, including $p21^{WAF1}$ and $p15^{NIK4B}$.[13] The cyclin-CDK complexes are inhibited *via* binding to CDK inhibitors.[14] Recently, the relationship

between cell cycle arrest and cancer has been emphasized by increasing evidence which suggests that the related processes of neoplastic transformation, progression and metastasis involve alterations of normal cell cycle regulation. Therefore, agents with anticancer (chemo-preventive) properties might affect the regulation of the cell-cycle machinery, resulting in cellular arrest at different phases of the cell cycle transition and thus reducing the growth and proliferation of cancerous cells, which might be useful in cancer therapy.

Currently, leukemia is among the most threatening diseases. As most adult leukemia patients are not candidates for transplantation and a more rational therapy has not been adequately defined, the patients are typically treated with regimens based on (or including) chemotherapy.[15,16] In our previous study, we demonstrated that the fermented broth of submerged *Antrodia camphorata* cultures had an apoptotic effect on human premyelocytic leukemia (HL-60) cells.[17] However, the effects of AC on tumor cell cycle regulation and tumor regression remained poorly understood. Therefore, the present study aimed to investigate the anticancer effects of AC with regard to cell cycle arrest *in vitro* in cultured human premyelocytic leukemia HL-60 cells and tumor regression *in vivo* in an athymic nude mouse model of leukemia.

Materials and methods

Chemicals

Roswell Park Memorial Institute (RPMI-1640) medium, fetal bovine serum (FBS), glutamine and penicillin/streptomycin were obtained from GIBCO BRL (Grand Island, NY, USA). Rabbit polyclonal antibodies against cyclin E, cyclin B1, CDK2, CDC2, $p21^{WAF1}$, Fas, FasL, caspase-8, and β-actin were purchased from Santa Cruz Biotechnology Inc. (Heidelberg, Germany). Mouse monoclonal antibodies against cyclin D1, CDK4, cyclin A, and Rb, a rabbit monoclonal antibody against p-Rb, and a rabbit polyclonal antibody against $p15^{INK4B}$ were obtained from

Cell Signaling Technology Inc., (Danvers, MA, USA). 3,3′-Dihexyloxacarbocyanine iodide ($DiCO_6$) was purchased from Invitrogen (Carlsbad, CA, USA). All other chemicals were either reagent or HPLC-grade and were supplied by either Merck (Darmstadt, Germany) or Sigma-Aldrich (St. Louis, MO, USA).

Preparation of the fermented broth from submerged *Antrodia camphorata* cultures

The strain of the fungus *Antrodia camphorata* was collected in Nantou County, Taiwan. The fungus was identified by Dr. Shy-Yuan Hwang of Endemic Species Research Institute, Nantou, Taiwan. Voucher specimen (CMU-AC010) have been deposited in China Medical University, Taichung, Taiwan. The hyphae of *Antrodia camphorata* was separated from the fruiting bodies. An *Antrodia camphorata* culture was inoculated on potato dextrose agar and incubated at 30 °C for 15–20 days. The entire colony was then placed in a flask containing 50 mL of sterile water. After homogenization, the fragmented mycelial suspension was used as an inoculum. The seed culture was prepared at 30 ºC in a 20 L fermenter (BioTop Processes & Equipment, Taichung, Taiwan) that was agitated at 150 rpm with an aeration rate of 0.2 vvm. Next, 15 L of a 5-day mycelium inoculum culture was inoculated into a 250-L agitated fermenter (BioTop). The fermentation conditions were the same as those used for the seed fermentation except for the aeration rate, which was 0.075 vvm. The fermentation product was harvested at hour 331 and filtered through non-woven fabric on a 20-mesh sieve to separate the deep-red fermented culture broth from the mycelia; the broth was centrifuged at 3000 × *g* for 10 min followed by passage through a 0.2-μm filter. The culture broth was concentrated under vacuum and freeze-dried to a powder. The yield of dry matter from the culture broth was 18.4 g/L. To prepare the stock solution, the powdered samples were solubilized in DMEM containing 1% FBS (pH 7.4). The stock solution (1.6 mg/mL) was stored at -20 °C prior to the evaluation of its anticancer properties. The experiments were performed with 2–4 different batches of the fermented

Antrodia camphorata culture.[18] The HPLC profile of the fermented culture broth of *Antrodia camphorata* was performed as previously described.[18] We will refer to the fermented *Antrodia camphorata* culture broth as AC throughout the manuscript.

Cell culture and cell viability assay

The human acute premyelocytic leukemia (HL-60) cell line was obtained from The American Type Culture Collection (ATCC; Rockville, MD, USA). Cells were grown in RPMI-1640 supplemented with 10% FBS, 2 mM glutamine, and 1% penicillin/streptomycin/neomycin in a 5% CO_2 humidified incubator at 37 °C. The cultures were harvested and cell numbers were counted using a hemacytometer. To determine the cell viability, cells were plated at a density of 2×10^5 cells/well in a 12-well plate and incubated with increasing concentrations of AC (20–80 μg/mL) for 24 h. After the 24-h incubation, the numbers of viable cells were quantified according to the trypan blue exclusion method. Prior to the trypan blue exclusion assay, the morphologies of the treated cells were photographed *via* phase contrast microscopy (200× magnification).

Flow cytometric analysis

The cellular DNA content was determined during a flow cytometric analysis of propidium iodide (PI)-labeled cells as described previously.[16] Briefly, HL-60 cells (2×10^5 cells/dish) were cultured in a 6-cm dish. After AC treatment (20–80 μg/mL) for 6–24 h, the cells were harvested, washed and suspended in phosphate-buffered saline (PBS) and were subsequently fixed overnight in ice-cold 70% ethanol at -20 °C. After the overnight incubation, the cells were re-suspended in PBS containing 1% Triton X-100, 0.5 mg/mL of RNase, and 4 μg/mL of PI at 37 °C for 30 min. A FACSCalibur flow cytometer (Becton Dickinson, San Jose, CA, USA) equipped with a single argon-ion laser (488 nm) was used for the flow cytometric analysis. The

forward and side-angle light scatter, which correlate with the cell size and cytoplasmic granularity, respectively, were used to establish the size gates and exclude cellular debris from the analysis. The DNA contents were determined for 1×10^4 cells per analysis. The cell-cycle pattern was determined using ModFit software (Verity Software House, Topsham, ME, USA). Apoptotic nuclei were identified as subploid DNA peaks and were distinguished from cell debris on the basis of the forward light scatter and PI fluorescence signals.

Protein isolation and western blot analysis

HL-60 cells (2×10^6 cells/dish) were seeded onto 10-cm dishes and incubated with increasing concentrations of AC (20–80 μg/mL) for 6–24 h. After the AC treatment, the whole cell lysate was obtained using standard lysis buffer. The total protein contents were determined using a protein assay reagent (Bio-Rad) and bovine serum albumin as the protein standard. Equal amount of were separated by SDS-PAGE and transferred overnight to PVDF membranes. The membranes were subsequently blocked with 5% non-fat skim milk for 30 min at room temperature, incubated overnight with specific primary antibodies, and then incubated with a horseradish peroxidase (HRP)-conjugated anti-rabbit or anti-mouse antibody for 2 h; the membranes were then developed with the SuperSignal ULTRA chemiluminescence substrate (Pierce Biotechnology, Rockford, IL, USA). Densitometric analyses were performed using a commercially available quantitative software package (AlphaEase, Genetic Technology Inc., Miami, FL, USA) with the control set to 1.0-fold as indicated below the western blot image.

Single-cell electrophoresis assay (Comet assay)

The comet assay is an uncomplicated and sensitive technique for detecting DNA damage at the level of an individual eukaryotic cell.[19] The comet assay was performed according to previously published guidelines.[20] Briefly, HL-60 cells (2×10^5 cells/dish in 6-cm dishes) were

incubated with increasing concentrations of AC (20–80 μg/mL) for 24 h. The cells were then suspended in 1% low-melting-point agarose in PBS (pH 7.4) and pipetted onto superfrosted glass microscope slides that had been pre-coated with a layer of 1% normal melting point agarose (which had been warmed to 37 °C prior to use). The agarose was allowed to set at 4 °C for 10 min, after which the slides were immersed in a lysis solution containing 2.5 M NaCl, 100 mM EDTA, 10 mM Tris, and 1% Triton X-100 at 4 °C for 1 h. The slides were then placed in single rows inside a 30-cm wide horizontal electrophoresis tank containing 0.3 M NaOH and 1 mM EDTA (pH 13.4) at 4 °C for 40 min to allow the separation of the two DNA strands (alkaline unwinding). Electrophoresis was performed in the unwinding solution at 30 V (1 V/cm) and 300 mA for 30 min. The slides were then washed three times for 5 min per wash with 0.4 M Tris (pH 7.5) at 4 °C prior to staining with propidium iodide (PI; 2.5 μg/mL). Observations were made at a final magnification of 200× on a UV microscope with a 435-nm excitation filter. Visual scoring of the cellular DNA on each slide was based on the characterization of 100 randomly selected nucleoids. Comet-like DNA formations were categorized into five classes (0, 1, 2, 3, or 4) that indicated increasing DNA damage in the form of a "tail". Each comet was assigned a value according to its class. The overall scores for 100 comets ranged from 0 (100% of comets received class 0 scores) to 400 (100% of comets received class 4 scores), and the overall DNA damage in the cell population was expressed in arbitrary units.[21] The observation and results analysis were always performed by the same experienced observer. This observer was blinded and had no knowledge about the identity of each slide. Cellular DNA damage was defined as DNA strand breaks, including double and single-strand variants at alkali-labile sites, and was analyzed under alkaline conditions (pH 13.4).

Analysis of mitochondrial membrane potential

Losses in mitochondrial membrane potential (ΔΨm) were assessed *via* flow cytometry. Briefly, HL-60 cells (2×10^5 cells/dish in a 6-cm dish) were incubated with AC (60 μg/mL) for 6–24 h. After AC treatment, the cells were harvested and washed twice with PBS, resuspended in 500 μL of $DiOC_6$ (4 M), and incubated at 37 °C for 30 min. The mitochondrial membrane potential was determined on a BD FACSCalibur cytometry system (BD Biosciences, Franklin Lakes, NJ, USA) with a 488-nm excitation wavelength and 530-nm bandpass emission filters ($DiOC_6$). Fluorescence was measured on the P2 (green) channel, gating only on live cells. The percentage of membrane potential was calculated using ModFit software (Verity Software, ME, USA).

Measurement of ROS generation

Intracellular ROS accumulation was detected *via* flow cytometry with 2′,7′-dihydrofluorescein-diacetate ($DCFH_2$-DA), a cell-permeable fluorogenic probe. HL-60 cells (2×10^5 cells/dish) were seeded into 6-cm dishes and allowed to reach approximately 80% confluence. To evaluate ROS generation in a time-dependent manner, the cells were treated with AC (60 μg/mL) for 15–60 min. After treatment, the culture supernatants were removed and the cells were then incubated with 10 μM $DCFH_2$-DA in fresh medium at 37 °C for 30 min. ROS production was measured according to changes in the fluorescence due to the intracellular accumulation of chlorofluorescein (DCF), which is caused by the oxidation of $DCFH_2$. ROS generation was measured on a BD FACSCalibur cytometry system (BD Biosciences) with a 15-milliwatt argon ion laser at 488 nm. The fluorescence was measured in the FL1 (green) channel after gating on live cells alone.

VEGF release assay

VEGF secretion by HL-60 cells was determined with a commercially available ELISA EIA kit

(Chemicon International Inc., Temecula, CA, USA). Briefly, HL-60 cells (1×10^5 cells/well were cultured in a 12-well plate. After reaching 85% confluence, the cells were treated with 20–80 μg/mL of AC for 24 h. The medium was then aspirated from the plates and centrifuged at 500 × *g* for 10 min to remove the cells. The concentration of VEGF that had been released into the culture medium was then estimated and reported in units of pg/10^5 cells.

Animals

Eight-week-old athymic nude mice (BALB/*c*-*nu*) were purchased from GlycoNex Inc. (Taipei, Taiwan) and maintained in separate cages in a specifically designed pathogen-free isolation facility with a 12-h light/dark cycle; the mice were provided rodent chow (Oriental Yeast Co, Tokyo, Japan) and water *ad libitum*. All experiments were conducted in accordance with the guidelines of the China Medical University Animal Ethics Research Board.

Tumor cell inoculation

HL-60 cells were grown in RPMI-1640 medium supplemented with 10% FBS. All experiments were performed with cells that had undergone fewer than 15 passages. HL-60 cells (1×10^6 cells in 200 μL of matrix gel) were injected subcutaneously into the right hind flanks of the nude mice as described previously.[22] Study groups II and III received intraperitoneal injections of 80 mg/kg and 120 mg/kg of AC, respectively, in 0.2 mL of PBS thrice weekly for 3 weeks; the control group (group I) received the vehicle alone (PBS) according to the same dosing schedule. To monitor drug toxicity, the body weight of each animal was measured every 3 days for 21 days. The tumor volume was determined every 3 days from caliper measurements of the tumor length, width and depth, according to the following formula: length × width^2 × 0.5.[23] The tumor volumes in each group of mice were noted once every 3 days for 21 days. After 3 weeks (21 days) of treatment, the mice were sacrificed. The tumors were removed and weighed prior

to fixation in 4% paraformaldehyde, sectioning and staining with hematoxylin-eosin, followed by light microscopic analysis. In addition, a pathologist examined the mouse organs, including the liver, lungs, and kidneys, for any possible drug side effects.

Histocytological analysis

A veterinary pathologist analyzed the tumor tissue sections for evidence of mitotic cells (proliferation) after AC treatment (80 and 120 mg/kg) and in comparison to sections from control animals. The biopsied tumor tissues were embedded in paraffin and cut into 3-mm-thick sections, placed in plastic cassettes and immersed in neutral buffered formalin for 24 h. The fixed tissues were deparaffinized and rehydrated using standard techniques. The extent to which AC treatment shrunk the tumor cells was evaluated by assessing the morphological and intracellular changes in hematoxylin and eosin-stained tumor sections.

Statistical analysis

The results of the *in vitro* and *in vivo* experiments are presented as the mean and standard deviation (mean ± SD) or standard error (mean ± SE), respectively. All study data were analyzed using the analysis of variance (ANOVA) followed by Dunnett's test for pair-wise comparisons. Statistical significance was defined as $p < 0.05$ for all tests.

Results

AC treatment induces cytotoxicity in human premyelocytic leukemia (HL-60) cells

In the present study, we evaluated the cytotoxic effects of *Antrodia camphorata* (AC) on human premyelocytic leukemia (HL-60) cells. The results from the trypan blue exclusion analysis revealed that AC treatment (20–80 μg/mL for 24 h) significantly and dose-dependently induced cell death with an IC_{50} value of 50.1 μg/mL (Fig. 1A). In addition, exposure to AC

induced significant HL-60 cell shrinkage, as determined by phase-contract microscopy (Fig. 1B). These primary data provided positive evidence that in HL-60 cells, AC treatment decreased the proliferation rate and induced cell death.

AC induces G_1 cell cycle arrest in HL-60 cells

In this study, we demonstrated that AC significantly inhibited HL-60 cell growth. To determine whether AC induced cell cycle arrest in HL-60 cells, the cells were treated with increasing concentrations of AC (20–80 μg/mL) for 6–24 h and were then subjected to a flow cytometric analysis after undergoing propidium iodide (PI) staining for DNA labeling. Flow cytometric data histograms are shown in Fig. 2. As shown in Fig. 2A, the control cells exhibited a normal cell cycle progression pattern, whereas AC treatment (20–80 μg/mL) resulted in a dose-dependent increase in the G_1 phase and a noticeable decrease in the S phase after 24 h. In addition, AC treatment (60 μg/mL) resulted in a time-dependent increase in the cell population in the G_1 phase, whereas the percentage of the population in the S phase was significantly decreased (Fig. 2B), indicating a G_1 arrest and the apparent inhibition of DNA synthesis in response to AC treatment in HL-60 cells.

Furthermore, HL-60 cells with reduced DNA staining relative to their diploid analogs were considered apoptotic. A remarkable accumulation of subploid cells, which produced the so-called sub-G_1 peak, was noted in the populations that had been treated with AC (20–80 μg/mL) for 6–24 h, compared with the untreated group (Fig. 2A and B). These data implied that AC treatment not only induced arrest at G_1 transition phase but also might have induced apoptotic death in the HL-60 cells.

AC downregulates cyclin D1, CDK4, cyclin E, CDK2, cyclin A, and pRb expression in HL-60 Cells

To examine the possible molecular mechanism(s) that might underlie changes in the cell cycle patterns, the effects of AC on various cyclins and cyclin-dependent kinases (CDKs) involved in HL-60 cell cycle arrest were investigated. Our investigative approach included treating the HL-60 cells with AC (20–80 μg/mL) for 6–24 h. Dose and time-dependent reductions in cyclin D1, CDK4, cyclin E, CDK2, and cyclin A expression were observed after AC treatment (Fig. 3A). However, AC treatment did not appear to affect the amounts of detectable cyclin B1 and CDC2 protein in the HL-60 cells (Fig. 3A); this finding was important because cyclin B1 and CDC2 form a complex that plays a major role in cellular entry into mitosis.

Because Rb regulates cell cycle progression, we therefore examined whether AC treatment would prevent Rb phosphorylation as a factor of its growth-inhibitory effects in HL-60 cells. Western blot analyses revealed that the levels of Rb and pRb were reduced in a dose- and time-dependent manner after AC treatment (Fig. 3A). These data suggested that AC treatment potentially arrested the G_1-S transition in HL-60 cells as evidenced by the downregulation of cyclin and CDK expression.

AC treatment increases $p21^{WAF1}$ and $p15^{INK4B}$ expression in HL-60 cells

The cyclin-dependent kinase inhibitors (CKIs) also play important roles in cell cycle progression. CKIs forms complexes with CDKs and thus prevent the activation of CDKs and the formation of CDK-cyclin complexes.[24] Therefore, we sought to examine whether AC treatment could modulate the expression levels of CKIs, including $p21^{WAF1}$ and $p15^{INK4B}$. As shown in Fig. 3B, AC treatment (20–80 μg/mL) for 6–24 h significantly increased the expression levels of $p21^{WAF1}$ and $p15^{INK4B}$ in the HL-60 cells a dose- and time-dependent manner. These data suggested that the AC-induced downregulation of CDKs might be due to induced CKI expression.

AC treatment induces apoptosis *via* DNA damage in HL-60 cells

DNA damage, represented by DNA single-strand breaks, was indicated by an increase in tail lengths. DNA damage was evaluated with the comet assay, in which the tail length is an important quantitative parameter. Therefore, the effect of AC treatment (20–80 μg/mL for 24 h) on cellular DNA damage was evaluated in a single-cell gel electrophoresis comet assay. A total toxicity scale was generated while considering the comet lengths (Fig. 4A). Our results showed that a dose-dependent increase in comet length was observed after HL-60 cells were treated with AC for 24 h (Fig. 4B), clearly indicating that AC treatment enhanced DNA damage. These data suggested that AC treatment induced apoptotic cell death in HL-60 cells.

AC treatment induces mitochondrial dysfunction *via* ROS generation in HL-60 cells

Cellular apoptosis occurs through several molecular pathways. The best-characterized and most prominent pathways are the extrinsic and intrinsic pathways. In the intrinsic pathway (also known as the mitochondria-dependent pathway), apoptosis results from an intracellular event cascade in which the mitochondrial membrane potential plays a crucial role.[25] We therefore examined whether AC treatment could induce mitochondrial membrane damage in HL-60 cells. The cells were treated with AC (60 μg/mL) for 6–24 h, followed by $DiOC_6$ staining. The mitochondrial membrane potential was then analyzed using flow cytometry. AC treatment resulted in a significant loss of mitochondrial membrane potential, as indicated by the time-dependent increase in the number of polarized cells (forward peak shift) after AC treatment (Fig. 5A). Additionally, the histogram showed that the percentage of mitochondrial potential ($\Delta\Psi m$) was significantly reduced in a time-dependent manner after AC treatment (Fig. 5B).

Excess ROS generation has been well characterized as a damaging influence on the mitochondrial membrane, and these damaged mitochondria can trigger cellular apoptosis.[25] To determine whether the AC-induced mitochondrial membrane permeability was mediated by

ROS generation, we examined the effects of AC on ROS generation in HL-60 cells. Intracellular ROS generation was estimated using fluorescence spectroscopy with the fluorescent probe $DCFH_2$-DA. Incubation with AC (60 μg/mL) for 15–60 min induced a significant time-dependent increase in DCF fluorescence in the HL-60 cells (Fig. 5C). Taken together, these data suggest that AC treatment induced an early increase in intracellular ROS generation that might have occurred upstream of mitochondrial dysfunction and DNA damage.

AC-mediated Fas-associated apoptotic pathway activation

To assess whether AC treatment (20–80 μg/mL for 6-24 h) could promote apoptosis *via* a death receptor-associated pathway, the Fas and Fas ligand (FasL) protein levels in HL-60 cells were determined by western blot analysis. The results revealed that AC treatment appreciably stimulated both Fas and FasL expression in a dose- and time-independent manner (Fig. 6). Fas and FasL are well known to cleave caspase-8 from procaspase-8, and activated caspase-8 further stimulates caspase-3 *via* a mitochondrial-dependent or independent cascade.[26] Therefore, we verified whether AC could augment caspase-8 cleavage in HL-60 cells. The western blot results showed that AC treatment induced caspase-8 cleavage from procaspase-8 in a dose and time-dependent manner (Fig. 6).

AC treatment reduces VEGF production in HL-60 cells

A number of studies have shown that VEGF is among the most important angiogenic factors and is closely associated with neovascularization in human tumors. An ELISA was performed to analyze the effects of AC on VEGF secretion by HL-60 cells. As shown in Fig. 7, AC treatment dose-dependently inhibited the level of VEGF secreted by HL-60 cells. More precisely, control cells (without treatment) secreted detectable levels of VEGF into the serum-free culture media at an approximate concentration of 52 pg/10^5 cells; in contrast, treatment

with 20, 40, 60, and 80 μg/mL of AC for 24 h reduced the secreted VEGF concentrations to 50, 9, 3, and 2.2 pg/10^5 cells, respectively (Fig. 7).

AC treatment inhibits tumor growth in HL-60 xenografted nude mice

We also investigated the antitumor potential of AC in a HL-60 xenografted nude mice model. As shown in Fig. 8A, the effects of AC on body weight remained unchanged, regardless of the duration of the experiment. In addition, no signs of toxicity were observed (data not shown) in any of the nude mice. The time courses of HL-60 xenograft growth with AC (80 and 120 mg/kg) and without treatment (control) are shown in Fig. 8B. After tumor cell inoculation, the tumor volumes gradually increased in the control mice; in contrast, AC treatment significantly and dose-dependently suppressed tumor development in the nude mice (Fig. 8B).

In addition, at the end of the 21-day period, the HL-60 xenograft tumors were excised from each of the sacrificed mice and weighed. A tumor volume evaluation revealed that AC treatment was associated with significant growth inhibition in a dose-dependent manner (Fig. 9A). The average tumor weight in the control group was 2.6 ± 0.5 g, whereas treatment with 80 and 120 mg of AC significantly reduced the tumor weights to 1.1 ± 0.2 g and 0.1 ± 0.1 g, respectively (Fig. 9B). These data demonstrated that AC treatment effectively suppressed tumor growth in the xenografted mice. Furthermore, hematoxylin and eosin staining of the tumor tissues revealed abundant mitosis (proliferating cells) in the control group, whereas the numbers of mitosis-positive cells were significantly reduced in the sections from the AC-treated (80 and 120 mg/kg) mice (Fig. 10). These *in vivo* data strongly suggested that AC treatment exhibited antitumor activity in the HL-60 leukemia-xenografted nude mice, a finding that might have been due to the modulation of cell-cycle regulation and/or the induction of apoptosis. Furthermore, *in vivo* toxicity was also examined superficially during histological studies of the vital organs (data not shown). No signs of significant toxicity were observed after exposure to

120 mg/kg b.w. of AC. This suggests that no side effects occurred at this dose.

Discussion

Several studies have demonstrated the potential anticancer activities of herbal medicines or mixtures *in vitro* or *in vivo*. Differential cell cycle regulation and subsequent events that lead to apoptotic cell death account for the anticancer effects of some potential phytochemicals.[27] Our previous study demonstrated that AC could induce apoptotic cell death in cultured human premyelocytic leukemia HL-60 cells.[17] The present investigation was a parallel study that demonstrated the effects of AC on *in vivo* human leukemia tumor xenografts in nude mice as well as *in vitro* HL-60 cell culture models. A summary of our data suggests that AC treatment could effectively suppress HL-60 cell proliferation as demonstrated by growth inhibition and cell cycle arrest both *in vitro* and *in vivo*.

Cancer cell cycle disruption is a therapeutic target in the development of new anticancer drugs.[28] The results of the cell cycle analysis in the present study showed that AC treatment had a profound effect on cell cycle control such that the premyelocytic leukemia cells accumulated in the G_1 phase. Progression through the G_1 phase requires both the cyclin D-dependent CDK4/CDK6 and CDK2/cyclin E holoenzymes.[12] The CDK catalytic subunits CDK4 and CDK2 and their regulatory subunits cyclin D1 and cyclin E are believed crucial to the regulation of S-phase entry, which appears to define the restriction point in the late G_1 phase. Cyclin D expression is frequently dysregulated in human neoplasias and, therefore, agents that downregulate cyclin D expression might facilitate both neoplasia prevention and treatment.[29] Furthermore, cyclin E, a key cell-cycle regulator, was found to be overexpressed in primary carcinoma tissues.[30] Cyclin A is a particularly interesting cyclin family member because it can activate two different types of CDKs and functions during both S-phase and mitosis.[30] Cyclin A-associated protein kinase activity is critical for the G_1-to-S-phase transition and further entry

into the M-phase.[31] The results of this study implied that the cyclin D1, CDK4, cyclin E, cyclin A, and CDK2 expression levels were downregulated by AC, a finding that corroborates a possible G_1 block in the treated HL-60 cells. Growth stimulation-signaling pathway impairment has been shown to induce the expression of CDK inhibitors that bind and subsequently inhibit cyclin-CDK complex activity.[32] Our data clearly demonstrated that Rb and pRb were suppressed by AC. As Rb phosphorylation occurs during the late G_1 phase, the AC-mediated inhibition of Rb and pRb would explain the cell cycle arrest in the G_1 phase. Our study also demonstrated a lack of significant differences in cyclin B1 and CDC2 expression after AC treatment. The complex formed by the association of cyclin B1 and CDC2 was reported to play a major role in mitotic entry.[33] Cell cycle progression is also coordinated by the balance between the cellular concentrations of Cdk inhibitors, including $p21^{WAF1}$ and $p15^{NIK4B}$.[34,35] Our results suggested that AC treatment induced $p21^{WAF1}$ and $p15^{NIK4B}$ expression, thus accounting for a considerable portion of the reduction in CDK activity and the subsequent inhibition of cell-cycle progression. Taken together, these results suggest that the observed inhibition of HL-60 cell proliferation in response to AC treatment might result from cell cycle arrest during the G_1 phase.

Investigations have shown that apoptosis is controlled by both mitochondrial and membrane death receptor pathways. Our previous investigation demonstrated that AC treatment could induce apoptotic cell death in HL-60 cells that was associated with a loss of cell viability, internucleosomal DNA fragmentation, cytochrome *c* translocation, caspase-3 activation, poly ADP-ribose polymerase (PARP) degradation, and Bcl-2 and Bax dysregulation.[17] However, the involvement of other signaling mechanisms in AC-treated HL-60 cells such as death receptor-mediated apoptosis remained largely unknown. The membrane death receptor pathway is initiated by the binding of transmembrane death receptors, including Fas, FasL, TNFR1, and TRAIL, with their cognate extracellular ligands.[36] Ligand receptors recruit adaptor proteins

such as TRADD and FADD, which interact with and trigger the activation of caspase-8. Activated caspase-8 further cleaves or activates downstream effector caspases such as caspase-3.[37] The present study indicated that AC-induced apoptosis was associated with Fas and FasL upregulation and increased caspase-8 activation in HL-60 cells. An analysis of our data suggested that AC-induced apoptosis was controlled by both mitochondrial and membrane DR pathways.

Many anticancer drugs have been reported to generate ROS *via* oxidative stress and to induce apoptosis in cancer cells, whereas many inhibitors of apoptosis exhibit antioxidant activity.[38] Indeed, factors that cause or promote oxidative stress such as ROS production, lipid peroxidation and antioxidant gene downregulation have been shown to be involved in apoptotic processes.[38] Moreover, ROS induction has been reported to upregulate the activities of certain enzymes involved in the cell death pathway by inducing mitochondrial dysfunction.[39] We previously reported that AC treatment could induce intracellular ROS generation, thus reducing the mitochondrial membrane potential and triggering apoptosis in human breast and ovarian cancer cell lines.[40-41] These results were consistent with the findings of the present study, which revealed that AC treatment-induced apoptosis in HL-60 cells might have been due to the induction of ROS generation and the loss of mitochondrial membrane potential.

The angiogenic factor VEGF is produced by endothelial cells to support the growth of many types of solid tumors and acute leukemias. The inhibition of VEGF gene expression represents a novel approach to cancer therapy.[42] Many natural health products that inhibit angiogenesis also manifest other anticancer activities.[42] We previously reported that AC treatment inhibited VEGF expression in human breast cancer and murine melanoma cell lines.[2,43] In this study, we observed that AC treatment significantly inhibited VEGF activity in HL-60 cells. The inhibitory effect of AC on VEGF expression in HL-60 cells, therefore, might be an important mechanism in the regulation of tumor neovascularization, thus further contributing to the overall control of

tumor growth and progression.

Furthermore, tumor inhibition was observed after AC treatment in xenografted nude mice. Both the mean tumor volumes and weights were significantly reduced in response to AC. Experiments conducted with animals and circulating blasts from leukemia patients have yielded evidence suggesting that apoptosis also occurs in response to chemotherapy *in vivo*. Human acute leukemic cell lines (HL-60 cells) have proven particularly informative in studies of chemotherapy-associated apoptotic proteolytic events.[17] Moreover, in this study, the *in vivo* toxicity of AC was also determined superficially from body weight changes and histological studies of vital organs (data not shown); no apparent signs of significant negative effects were observed at dosages of 80 and 120 mg/kg. An analysis of our data suggests that AC exerted anti-proliferative and growth-inhibitory activities on HL-60 cells both *in vitro* and *in vivo*.

It is reasonable to suggest that the anticancer potential of AC might result from an abundance of bioactive components because AC metabolizes the culture medium and releases active components during fermentation, particularly polysaccharides, triterpenoids, steroids, benzenoids, and maleic/succinic acid derivatives.[3-5] The reported yields of polysaccharides, crude triterpenoids, and total polyphenols in the fermented AC broth were 23.2 mg/g, 47 mg/g, and 67 mg/g, respectively, whereas no polysaccharides, crude triterpenoids, or polyphenols were detected in the dry matter from the culture medium.[1] The chemical profile and major constituents of the wild type and fermented culture broth of AC are similar, but the biological activity of any natural product depends on the synergistic and antagonistic activity of the whole spectrum of its active ingredients.[5] In our previous study, we isolated 2,3-dimethoxy-5-methyl-1,4-benzoquinone [17.3% (254 nm) and 13.5% (220 nm)] from the fermented culture broth of AC, as determined by HPLC.[18] In addition, a previous study showed that rats treated with AC (500 mg/kg/day *via* oral) for 28 days did not display any lethal effects or toxic signs, thus supporting the potential of this agent for food and drug applications.[44] In the present study, we

also superficially evaluated the toxic effects of AC using body weight changes and histological studies of vital organs (data not shown). There appeared to be no signs of significant toxicity at AC exposures up to 120 mg/kg. This finding likely indicates a lack of side effects at these doses. However, further studies are warranted to determine the optimal/effective AC dose.

The results obtained from the *in vitro* and *in vivo* studies implied that *Antrodia camphorata* could act as a chemopreventive agent with respect to human leukemia HL-60 cell growth inhibition mediated through cell cycle arrest and apoptosis. These data provide important information that might contribute to a model of the effects of *Antrodia camphorata* for potential future studies with large animal models and human patients and might thereby facilitate the development of nutraceutical products from this agent.

Acknowledgements

This work was supported by grants NSC-101-2320-B-039-050-MY3, CMU 100-ASIA-13, and CMU 100-ASIA-14 from the National Science Council, Asia University, and China Medical University of Taiwan, respectively. The authors have no conflicts of interest to declare.

References

1 Y. C. Hseu, W. C. Chang, Y. T. Hseu, C. Y. Lee, Y. J. Yech, P. C. Chen, J. Y. Chen and H. L. Yang, Protection of oxidative damage by aqueous extract from *Antrodia camphorata* mycelia in normal human erythrocytes, *Life Sci.*, 2002, 71, 469-482.

2 Y. C. Hseu, H. T. Tsou, K. J. S. Kumar, K. Y. Lin, H. W. Chang and H. L. Yang, The antitumor activity of *Antrodia camphorata* in melanoma cells: Modulation of wnt/beta-catenin signaling pathways, *Evid. Based Complement Alternat. Med.,* 2012, 197309.

3 Z. H. Ao, Z. H. Xu, Z. M. Lu, H. Y. Xu, X. M. Zhang and W. F. Dou, Niuchangchih (*Antrodia camphorata*) and its potential in treating liver diseases, *J. Ethnopharmacol.,* 2009,

121, 194-212.

4 M. Geethangili and Y. M. Tzeng, Review of pharmacological effects of *Antrodia camphorata* and its bioactive compounds. *Evid. Based Complement Alternat. Med.*, 2011, 212641.

5 M. C. Lu, M. El-Shazly, T. Y. Wu, Y. C. Du, T. T. Chang, C. F. Chen, Y. M. Hsu, K. H. Lai, C. P. Chiu, F. R. Chang and Y. C. Wu, Recent research and development of *Antrodia cinnamomea*, *Pharmacol. Ther*., 2013, 139, 124-156.

6 P. Y. Yue, Y. Y. Wong, T. Y. Chan, C. K. Law, Y. K. Tsoi and K. S. Leung, Review of biological and pharmacological activities of the endemic Taiwanese bitter medicinal mushroom, *Antrodia camphorata* (M. Zang et C. H. Su) Sh. H. Wu et al. (higher Basidiomycetes), *Int. J. Med*., 2012, 14, 241-256.

7 M. F. Wu, F. C. Peng, Y. L. Chen, C. S. Lee, Y. Y. Yang, M. Y. Yeh, C. M. Liu, J. B. Chang, R. S. Wu, C. C. Yu, H. F. Lu and J. G. Chung, Evaluation of genotoxicity of *Antrodia cinnamomea* in the Ames test and the *in vitro* chromosomal aberration test, *In Vivo*., 2011, 25, 419-423.

8 N. Ahmad, V. M. Adhami, F. Afaq, D. K. Feyes and H. Mukhtar, Resveratrol causes WAF-1/p21-mediated G(1)-phase arrest of cell cycle and induction of apoptosis in human epidermoid carcinoma A431 cells, *Clin. Cancer Res*., 2001, 7, 1466-1473.

9 C. A. Schmitt, Senescence, apoptosis and therapy--cutting the lifelines of cancer, *Nat. Rev. Cancer*., 2003, 3, 286-295.

10 Z. A. Stewart, M. D. Westfall and J. A. Pietenpol, Cell-cycle dysregulation and anticancer therapy, *Trends Pharmacol. Sci*., 2003, 24, 139-145.

11 J. Bloom and F. R. Cross, Multiple levels of cyclin specificity in cell-cycle control, *Nat. Rev. Mol. Cell Biol*., 2007, 8, 149-160.

12 A. Takahashi, T. Taniguchi, Y. Ishikawa and M. Yokoyama, Tranilast inhibits vascular

smooth muscle cell growth and intimal hyperplasia by induction of p21(waf1/cip1/sdi1) and p53, *Circ. Res*., 1999, 84, 543-550.

13 W. C. Weinberg and M. F. Denning, P21Waf1 control of epithelial cell cycle and cell fate, *Crit. Rev. Oral. Biol. Med*., 2002, 13, 453-464.

14 L. Esposito, P. Indovina, F. Magnotti, D. Conti and A. Giordano, Anticancer therapeutic strategies based on CDK inhibitors, *Curr. Pharm. Des*., 2013, 19, 5327-5332.

15 E. H. Estey, Treatment of acute myeloid leukemia, *Haematologica*., 2009, 94, 10-16.

16 P. J. Huang, Y. C. Hseu, M. S. Lee, K. J. S. Kumar, C. R. Wu, L. S. Hsu, J. W. Liao, I. S. Cheng, Y. T. Kuo, S. Y. Huang and H. L. Yang, *In vitro* and *in vivo* activity of gallic acid and *Toona sinensis* leaf extracts against HL-60 human premyelocytic leukemia, *Food Chem. Toxicol*., 2012, 50, 3489-3497.

17 Y. C. Hseu, H. L. Yang, Y. C. Lai, J. G. Lin, G. W. Chen and Y. H. Chang, Induction of apoptosis by *Antrodia camphorata* in human premyelocytic leukemia HL-60 cells, *Nutr. Cancer*., 2004, 48, 189-197.

18 Y. C. Hseu, H. C. Huang and C. Y. Hsiang, *Antrodia camphorata* suppresses lipopolysaccharide-induced nuclear factor-kappaB activation in transgenic mice evaluated by bioluminescence imaging, *Food Chem. Toxicol*., 2010, 48, 2319-2325.

19 A. Dhawan, M. Bajpayee and D. Parmar, Comet assay: a reliable tool for the assessment of DNA damage in different models, *Cell Biol. Toxicol*., 2009, 25, 5-32.

20 N. P. Singh, M. T. McCoy, R. R. Tice and E. L. Schneider, A simple technique for quantitation of low levels of DNA damage in individual cells, *Exp. Cell Res*., 1988, 175, 184-191

21 L. Nousis, P. T. Doulias, N. Aligiannis, D. Bazios, A. Agalias, D. Galaris and S. Mitakou, DNA protecting and genotoxic effects of olive oil related components in cells exposed to hydrogen peroxide, *Free Radic. Res*., 2005, 39, 787-795.

22 Y. C. Hseu, C. S. Chen and S. Y. Wang, *Alpinia pricei* rhizome extracts induce cell cycle arrest in human squamous carcinoma KB cells and suppress tumor growth in nude mice, *Evid. Based Complement Alternat. Med*., 2011, 123815.

23 A Collins, L. Yuan, T. L. Kiefer, Q. Cheng, L. Lai and S. M. Hill, Overexpression of the MT1 melatonin receptor in MCF-7 human breast cancer cells inhibits mammary tumor formation in nude mice, *Cancer lett*., 2003, 189, 49-57.

24 V. Krystof and S. Uldrijan, Cyclin-dependent kinase inhibitors as anticancer drugs, *Curr. Drug Targets*., 2010, 11, 291-302.

25 G. Kroemer, L. Galluzzi and C. Brenner, Mitochondrial membrane permeabilization in cell death, *Physiol Rev*., 2007, 87, 99-163.

26 T. Imao and S. Nagata, Apaf-1- and Caspase-8-independent apoptosis, *Cell Death Differ*., 2013, 20, 343-352.

27 M. B. Sporn and N. Suh, Chemoprevention: an essential approach to controlling cancer, *Nat. Rev. Cancer*., 2002, 2, 537-543.

28 S. Diaz-Moralli, M. Tarrado-Castellarnau, A. Miranda and M. Cascante, Targeting cell cycle regulation in cancer therapy, *Pharmacol. Ther*., 2013, 138, 255-271.

29 E. A. Sausville, J. Johnson, M. Alley, D. Zaharevitz and A. M. Senderowicz, Inhibition of CDKs as a therapeutic modality, *Ann. N. Y. Acad. Sci*., 2000, 910, 207-221; discussion 221-202.

30 Y. Dong, L. Sui, Y. Tai, K. Sugimoto, T. Hirao and M. Tokuda, Prognostic significance of cyclin E overexpression in laryngeal squamous cell carcinomas, *Clin. Cancer Res*., 2000, 6, 4253-4258.

31 N. Furuno, N. den Elzen and J. Pines, Human cyclin A is required for mitosis until mid prophase, *J. Cell Biol*., 1999, 147, 295-306.

32 T. Sandal, Molecular aspects of the mammalian cell cycle and cancer, *Oncologist*., 2002, 7,

73-81.

33 P. L. Kuo, Y. L. Hsu and C. Y. Cho, Plumbagin induces G2-M arrest and autophagy by inhibiting the AKT/mammalian target of rapamycin pathway in breast cancer cells, *Mol. Cancer Ther*., 2006, 5, 3209-3221.

34 E. T. Canepa, M. E. Scassa, J. M. Ceruti, M. C. Marazita, A. L. Carcagno, P. F. Sirkin and M. F. Ogara, INK4 proteins, a family of mammalian CDK inhibitors with novel biological functions, *IUBMB. Life*., 2007, 59, 419-426.

35 J. Cicenas, and M. Valius, The CDK inhibitors in cancer research and therapy, *J. Cancer Res. Clin. Oncol*., 2011, 137, 1409-1418.

36 C. J. Reed, Apoptosis and cancer: strategies for integrating programmed cell death, *Semin. Hematol*., 2000, 37, 9-16.

37 D. Subramaniam, P. Giridharan, N. Murmu, N. P. Shankaranarayanan, R. May, C. W. Houchen, R. P. Ramanujam, A. Balakrishnan, R. A. Vishwakarma and S. Anant, Activation of apoptosis by 1-hydroxy-5,7-dimethoxy-2-naphthalene-carboxaldehyde, a novel compound from *Aegle marmelos*, *Cancer Res*., 2008, 68, 8573-8581.

38 T. Ozben, Oxidative stress and apoptosis: impact on cancer therapy, *J. Pharm. Sci*., 2007, 96, 2181-2196.

39 F. H. Chen, L. B. Zhang, L. Qiang, Z. Yang, T. Wu, M. J. Zou, L. Tao, Q. D. You, Z. Y. Li, Y. Yang and Q. L. Guo, Reactive oxygen species-mitochondria pathway involved in LYG-202-induced apoptosis in human hepatocellular carcinoma HepG(2) cells, *Cancer Lett*., 2010, 296, 96-105.

40 C. C. Lee, H. L. Yang, T. D. Way, K. J. S. Kumar, Y. C. Juan, H. J. Cho, K. Y. Lin, L. S. Hsu, S. C. Chen and Y. C. Hseu, Inhibition of cell growth and induction of apoptosis by *Antrodia camphorata* in HER-2/neu-overexpressing breast cancer cells through the induction of ROS, depletion of HER-2/neu, and disruption of the PI3K/Akt signaling pathway, *Evid. Based*

Complement Alternat. Med., 2012, 702857.

41 H. L. Yang, K. Y. Lin, Y. C. Juan, K. J. S. Kumar, T. D. Way, P. C. Shen, S. C. Chen and Y. C. Hseu, The anti-cancer activity of *Antrodia camphorata* against human ovarian carcinoma (SKOV-3) cells *via* modulation of HER-2/neu signaling pathway, *J. Ethnopharmacol*., 2013, 148, 254-265.

42 S. M. Sagar, D. Yance and R. K. Wong, Natural health products that inhibit angiogenesis: a potential source for investigational new agents to treat cancer, *Curr. Oncol*., 2006, 13, 14-26.

43 H. L. Yang, Y. H. Kuo, C. T. Tsai, Y. T. Huang, S. C. Chen, H. W. Chang, E. Lin, W. H. Lin and Y. C. Hseu, Anti-metastatic activities of *Antrodia camphorata* against human breast cancer cells mediated through suppression of the MAPK signaling pathway, *Food Chem. Toxicol*., 2011, 49, 290-298.

44 W. C. Lin, S. C. Kuo and Y. W. Wu, Effects of 28-day's repeated oral administration of the fermented extract of mycelia of *Antrodia comphorata* on rats. *J. Chin. Med*., 2001, 12, 293-303.

Figure Legends

Fig. 1 *Antrodia camphorata* (AC) treatment inhibits human premyelocytic leukemia (HL-60) cell growth. (A) HL-60 cells were treated with increasing concentrations of AC (20–80 μg/mL) for 24 h. Cell viability was determined before and after AC treatment according to the trypan blue exclusion method and phase-contrast microscopy. (B) HL-60 cells were treated with AC (20–80 μg/mL) for 24 h. The cell morphologies of AC-treated HL-60 cells were determined by phase-contrast microscopy at 200 × magnification. Each value is expressed as the mean ± SD (n=3). *Significant difference, compared with the control group ($p < 0.05$).

Fig. 2 AC treatment induces G_1–S cell-cycle arrest in HL-60 cells. (A) Cells were treated with increasing concentrations of AC (20–80 μg/mL) for 24 h, stained with PI, and analyzed by flow cytometry to determine the sub-G_1 population and cell cycle transition. (B**)** Cells were treated with AC (60 μg/mL) for 6–24 h, stained with PI, and analyzed by flow cytometry to determine the sub-G_1 population and cell cycle progression. The histogram shows the distributions (as percentages) of cells in the different cell cycle phases (sub-G_1, G_1, S, and G_2/M) after AC treatment. Apoptotic nuclei were identified by a subploid DNA peak and were distinguished from cell debris based on forward light scattering and PI fluorescence. The results are presented as the mean ± SD (n=3). *Significant difference, compared with the control group ($p < 0.05$).

Fig. 3 AC inhibits cell cycle regulatory protein expression in HL-60 cells. HL-60 cells were treated with increasing concentrations of AC (20–80 μg/mL) for 6-24 h (A and B). Protein samples (50 μg) were resolved on 10–12% SDS-PAGE gels and analyzed *via* western blotting. β-actin was used as an internal control. Relative changes in the protein bands (indicated below each western blot) were measured using commercially available quantitative software. A typical result from three independent experiments is shown.

Fig. 4 AC treatment induced DNA damage in HL-60 cells. HL-60 cells were treated with AC (20–80 μg/mL) for 24 h. (A) The comet-like DNA formations were categorized into five classes (0, 1, 2, 3, or 4) to indicate increasing DNA damage in the form of a "tail". Each comet was assigned a value according to its class. (B) The overall scores for 100 comets ranged from 0 (100% of comets with class 0 scores) to 400 (100% of comets with class 4 scores). The results are presented as the mean ± SD (n=3). *Significant difference, compared with the control group ($p < 0.05$).

Fig. 5 AC treatment induces mitochondrial dysfunction *via* intracellular ROS generation in HL-60 cells. (A) HL-60 cells were grown in the absence (control) or presence of AC (60 μg/mL) for 6–24 h, stained with $DiOC_6$, and analyzed using flow cytometry as described in the Materials and Methods section. Representative flow cytometric patterns are shown. (B) The percentage of mitochondrial membrane potential (ΔΨm) as indicated by $DiOC_6$ fluorescence after AC treatment. (C) HL-60 cells were treated with AC (60 μg/mL) for 15–60 min. The non-fluorescent cell membrane-permeable probe $DCFH_2$-DA (10 μM) was added to the culture medium 30 min prior to the end of each experiment. Upon permeating the cell membrane, $DCFH_2$-DA reacts with cellular ROS and is metabolized into fluorescent DCF, thus indicating ROS production in a manner that can be measured using flow cytometry. The intracellular ROS levels are expressed in the graph as a percentage of the control. The results are presented as the mean ± SD (n=3). *Significant difference, compared with the control group ($p < 0.05$).

Fig. 6 AC induces apoptosis *via* death-receptor pathway activation. HL-60 cells were treated with increasing concentrations of AC (20–80 μg/mL) for 6–24 h. Protein samples (50 μg) were resolved on 10–12% SDS-PAGE gels and analyzed by western blotting. β-actin was used as an

internal control. Relative changes in the protein bands (indicated below each western blot) were measured using commercially available quantitative software. A typical result from three independent experiments is shown.

Fig. 7 AC treatment inhibits VEGF expression in HL-60 cells. HL-60 cells were treated with increasing concentrations of AC (20–80 μg/mL) for 24 h. The VEGF concentrations in the culture medium were quantified using a commercially available assay kit as described in the Materials and Methods. The results are presented as the mean ± SD (n=3). *Significant difference, compared with the control group ($p < 0.05$).

Fig. 8 Time-course effect of AC on HL-60 xenograft growth in nude mice. HL-60 cells were implanted subcutaneously into the flanks of nude mice on day 0; the animals were subsequently treated with AC (80 and 120 mg/kg) or vehicle (control) thrice weekly for 3 weeks. Tumor development was determined according to body weight (A) and tumor volume (B) measurements that were performed every 3 days. The results are presented as the mean ± SD (n=3). *Significant difference, compared with the control group ($p < 0.05$).

Fig. 9 *In vivo* HL-60 xenograft tumor inhibition is mediated by AC. Nude mice were treated with AC (80 and 120 mg/kg) or vehicle (control) thrice weekly for 3 weeks. On the 21th day after tumor implantation, the animals were sacrificed and the tumors were removed. (A) Photographs displaying the tumor volumes before and after dissection. (B) Histogram indicating the tumor volumes (g/mice). The results are presented as the mean ± SD (n=3). *Significant difference, compared with the control group ($p < 0.05$).

Fig. 10 AC inhibits xenograft tumor growth *via* cell cycle arrest. Tumor tissues from control

and AC (80 and 120 mg/kg)-treated mice were sectioned, stained with hematoxylin and eosin, and examined *via* light microscopy (400× magnification). Arrows indicate the mitotic nuclei in the tumor cells (control) and the AC-induced (80 and 120 mg/kg) shrunken tumor cells. Typical results from one of three independent experiments are shown.

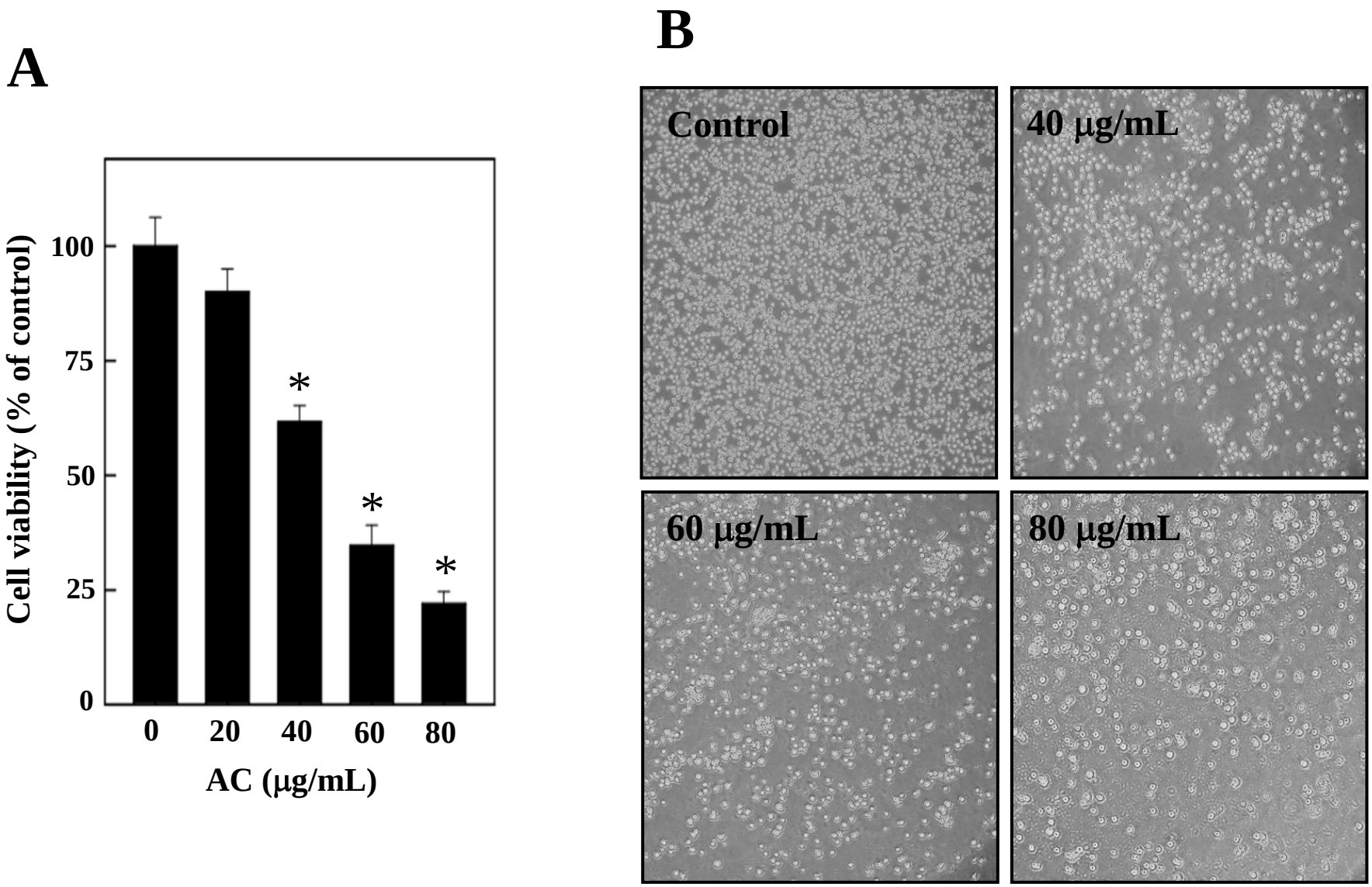

Fig 1

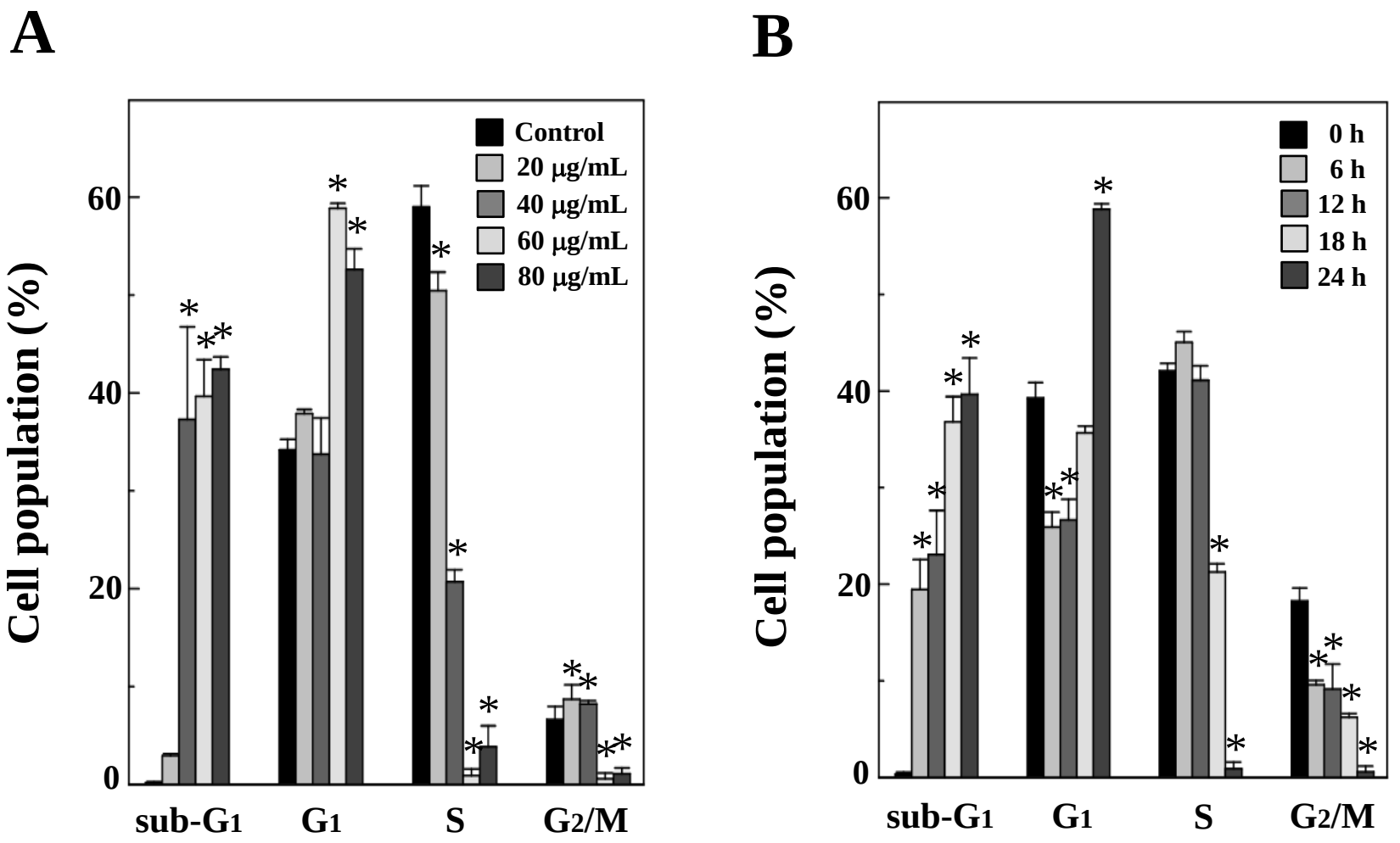

Fig 2

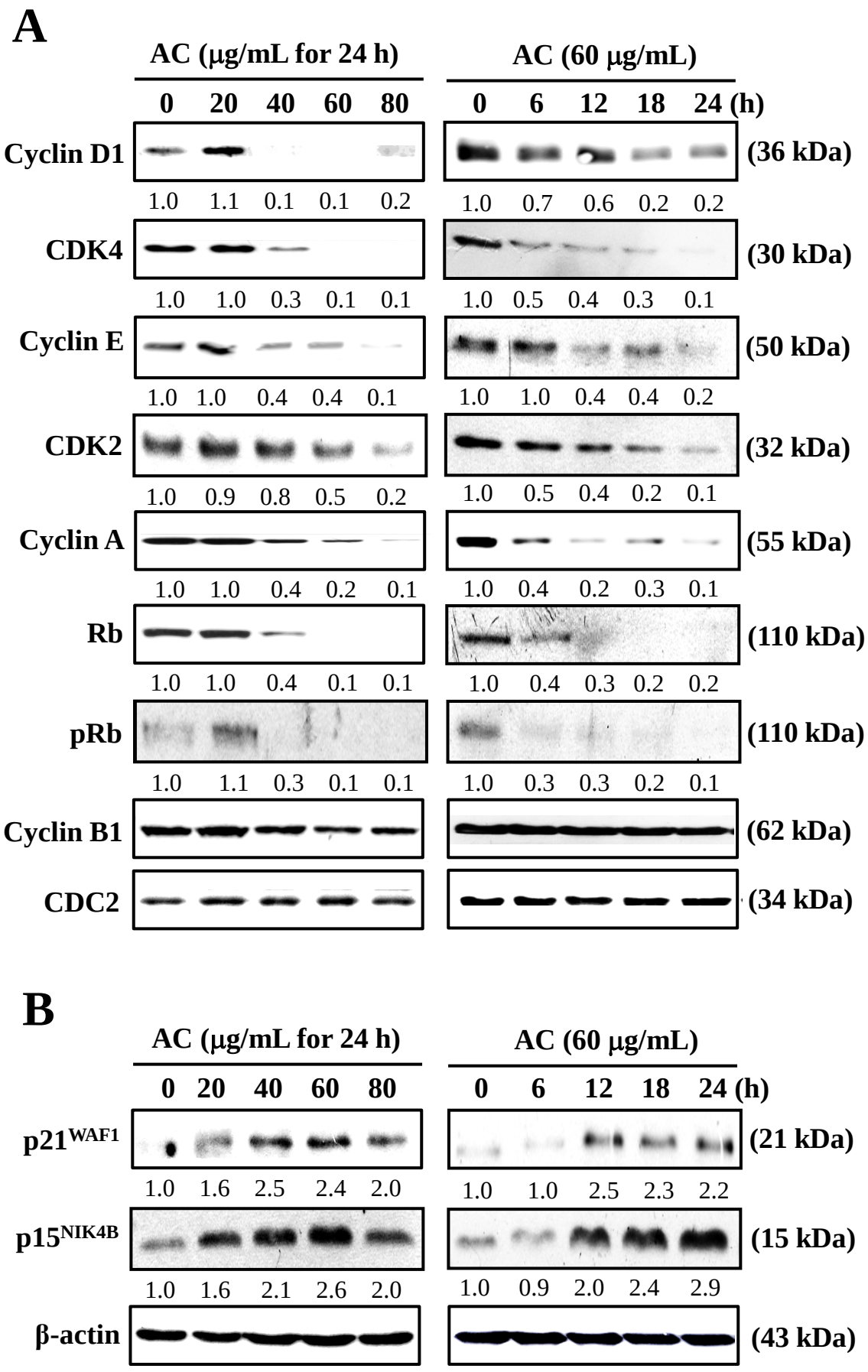

Fig 3

A

B

AC (μg/mL)	Toxicity scale					Total damage
	0	1	2	3	4	
0	96 ± 1	4 ± 1	1 ± 1	0 ± 0	0 ± 0	5 ± 2
20	57 ± 9	28 ± 7	13 ± 9	2 ± 1	0 ± 0	60 ± 19*
40	11 ± 3	16 ± 2	43 ± 5	30 ± 4	0 ± 0	191 ± 9*
60	0 ± 0	13 ± 7	39 ± 12	42 ± 10	6 ± 6	276 ± 15*
80	0 ± 0	1 ± 1	4 ± 3	25 ± 4	70 ± 4	362 ± 8*

Fig 4

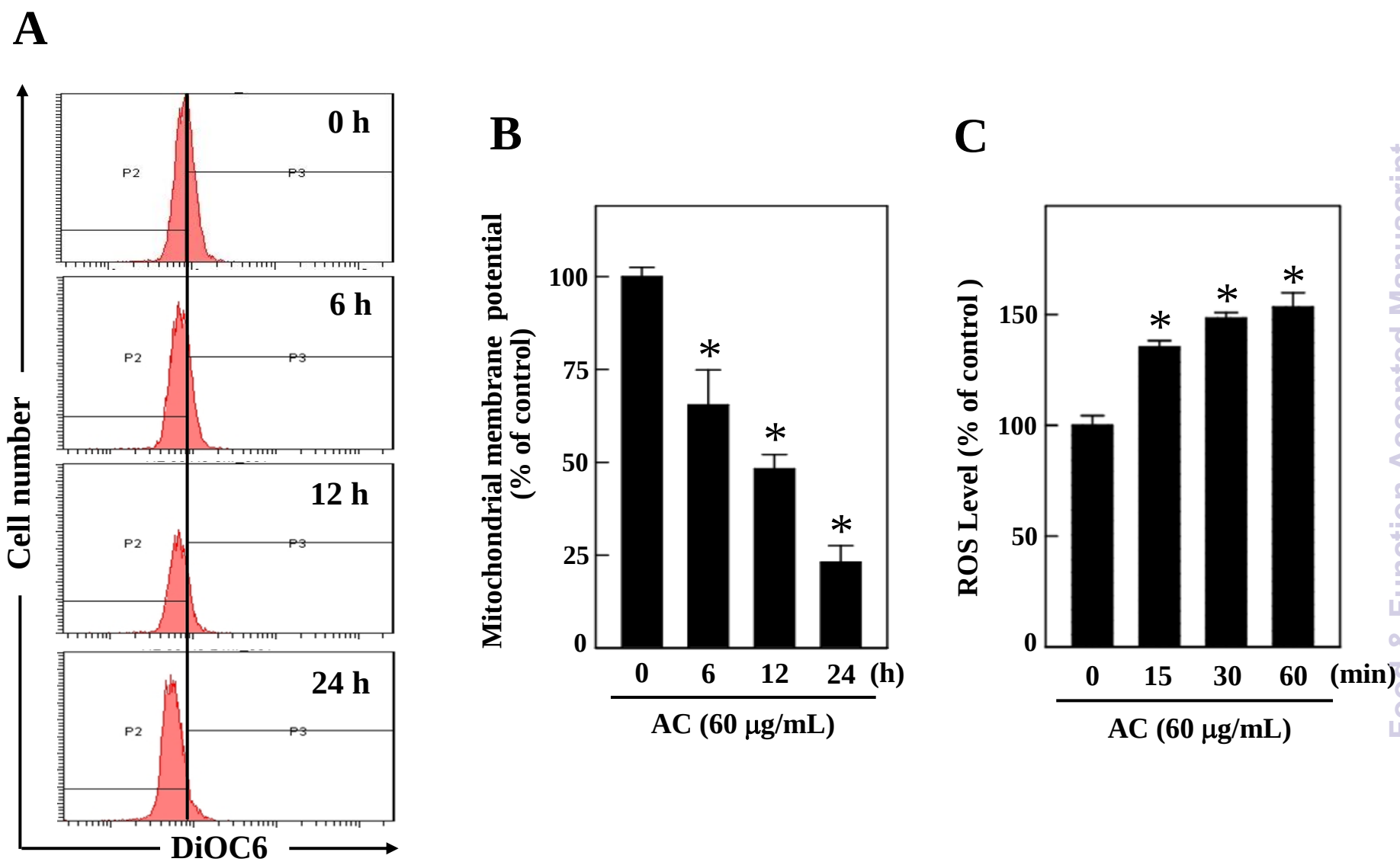

Fig 5

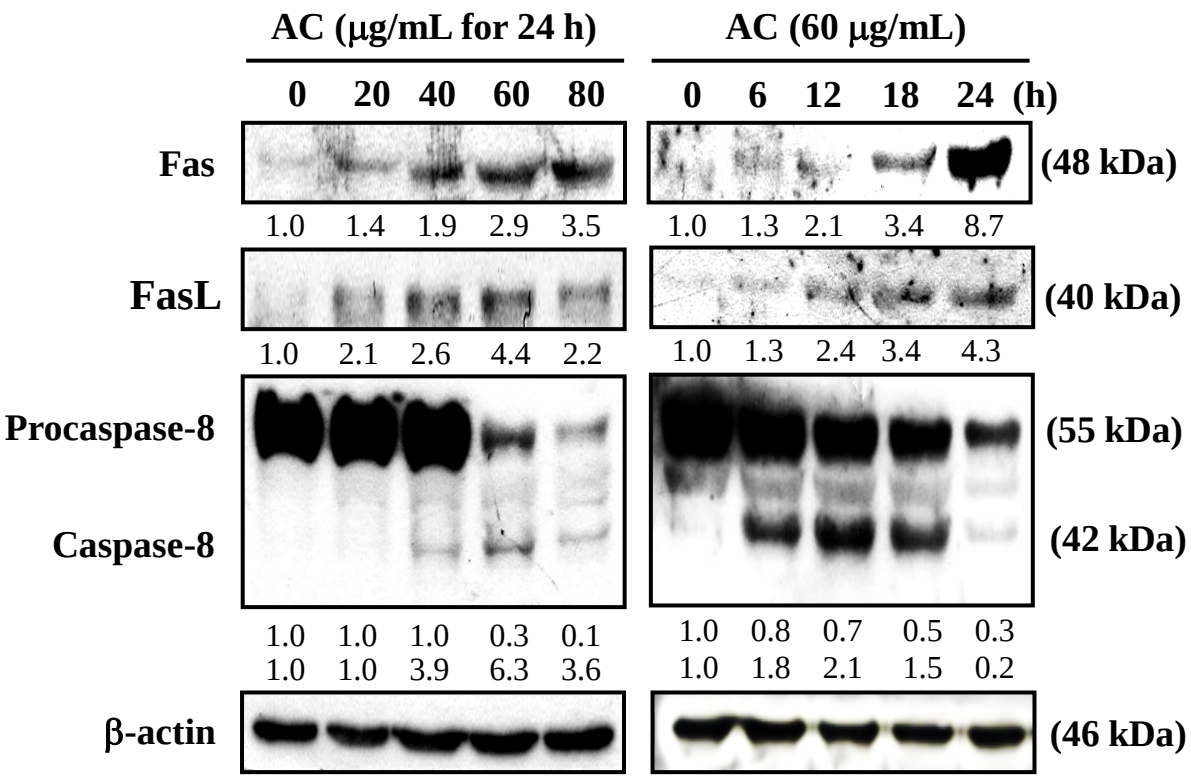

Fig 6

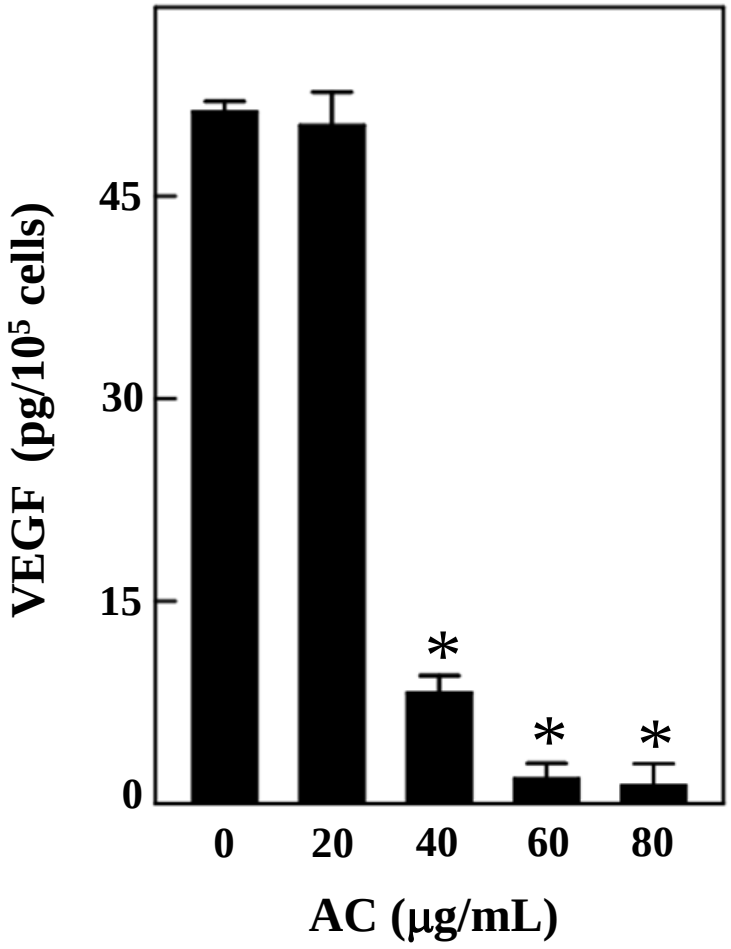

Fig 7

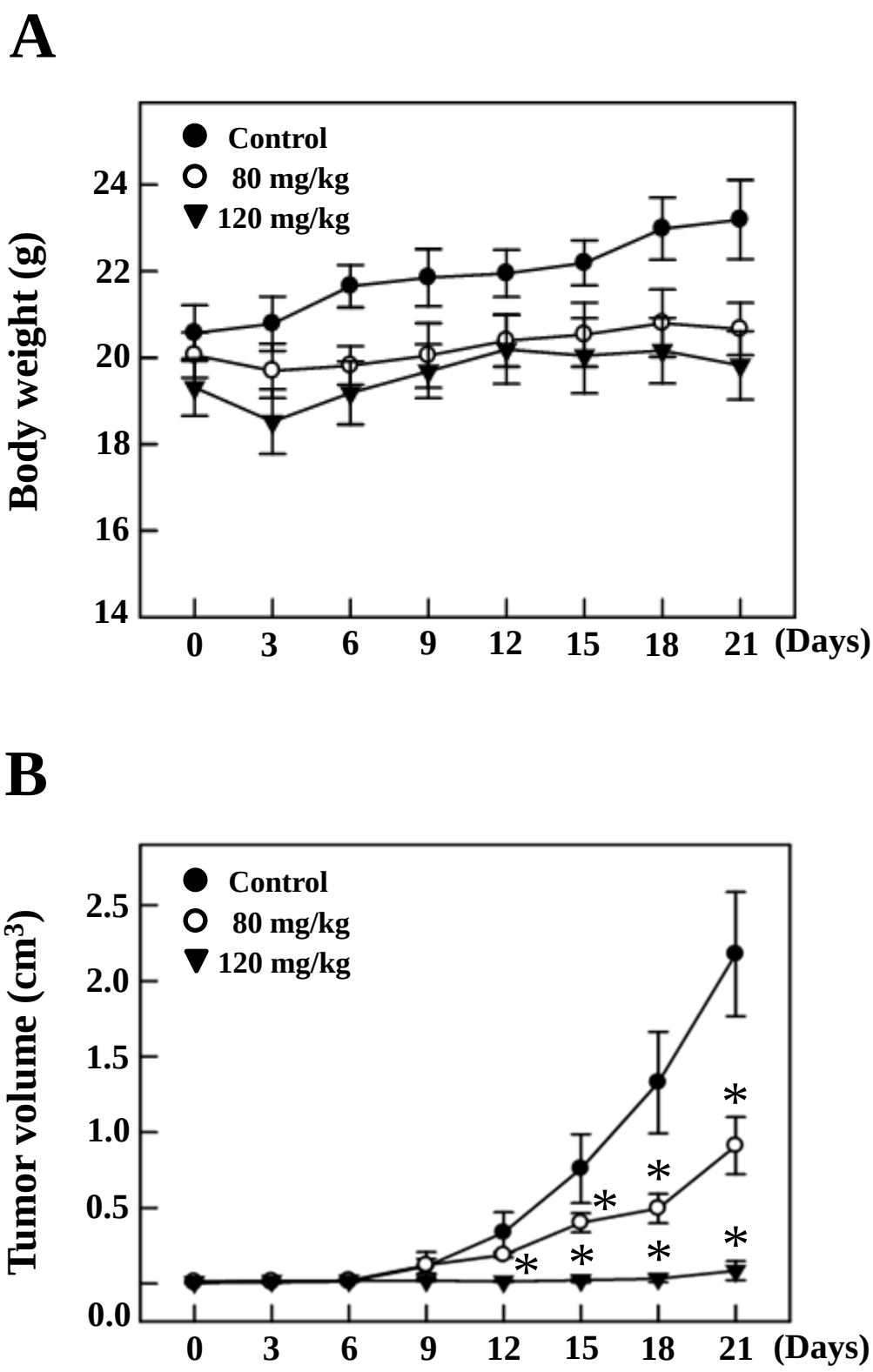

Fig. 8.

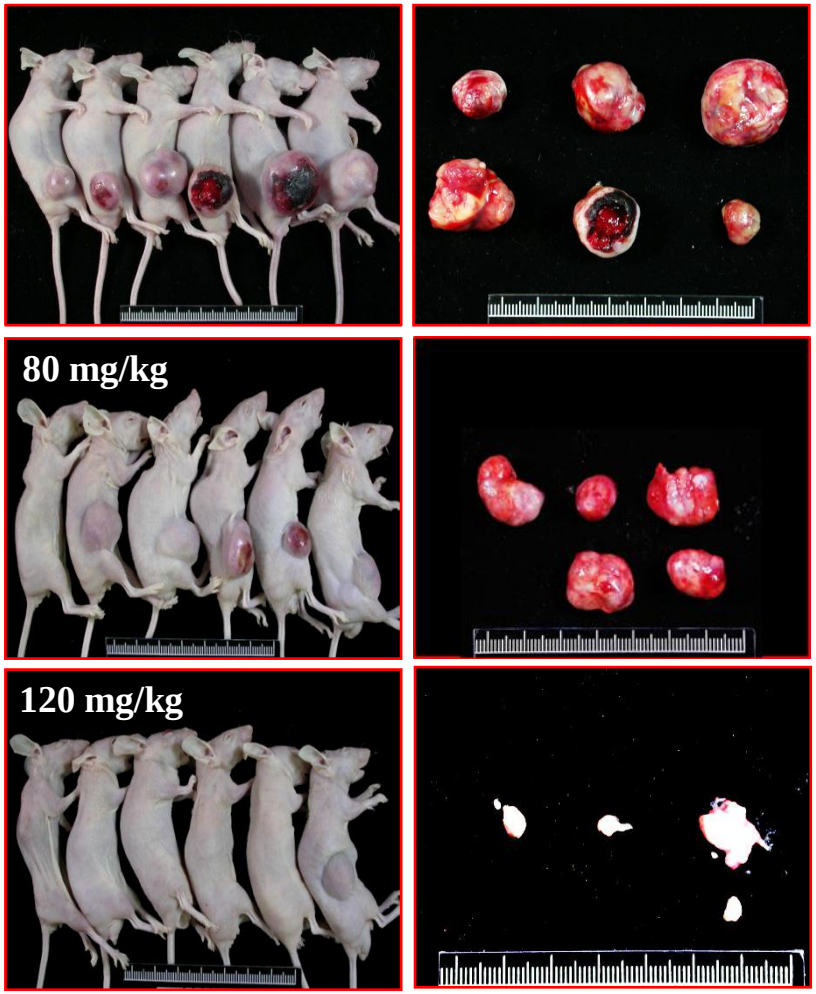

Fig 9

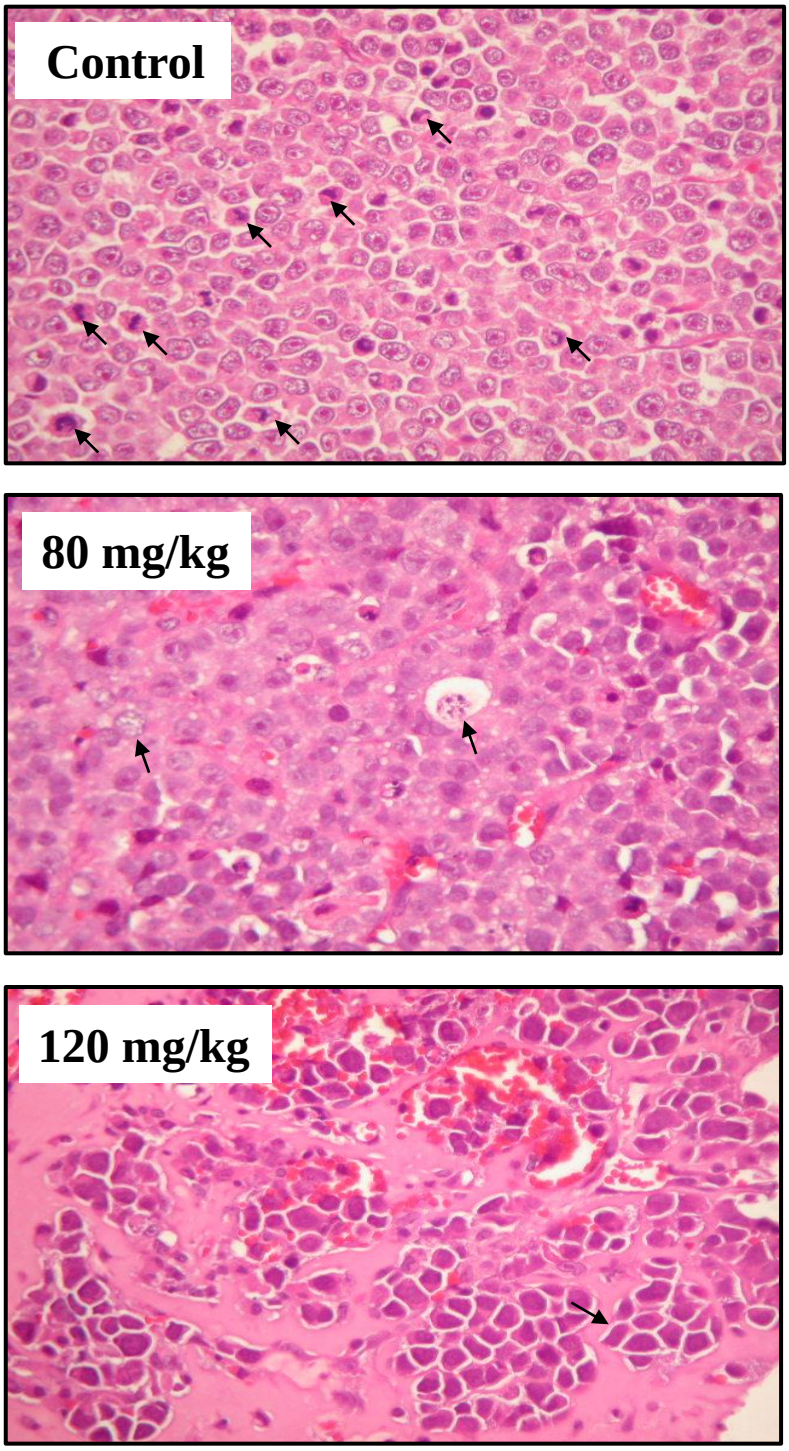

Fig. 10